Pré-Publicações do Departamento de Matemática
Universidade de Coimbra
Preprint Number 05–06

ACTUATOR EFFECT OF A PIEZOELECTRIC ANISOTROPIC PLATE MODEL

LINO COSTA, PEDRO OLIVEIRA, ISABEL N. FIGUEIREDO AND ROGÉRIO LEAL

Abstract: This paper addresses the actuator effect of a piezoelectric anisotropic plate model, depending on the location of the applied electric potentials, and for different clamped boundary conditions. It corresponds to integer optimization problems, whose objective functions involve the displacement of the plate. We adopt the two-dimensional piezoelectric anisotropic nonhomogeneous plate model derived in Figueiredo and Leal [1]. This model is first discretised by the finite element method. Then, we describe the associated integer optimization problems, which aim to find the maximum displacement of the plate, as a function of the location of the applied electric potentials. In this sense, we also introduce a related multi-objective optimization problem, that is solved through genetic algorithms. Several numerical examples are reported. For all the tests, the stiffness matrices and force vectors have been evaluated with the subroutines *planre* and *platre*, of the CALFEM toolbox of MATLAB [2], and, the genetic algorithms have been implemented in C^{++}.

Keywords: Piezoelectric Material, Plate, Finite Elements, Genetic Algorithms.

1. Introduction

Piezoelectric materials are characterized by the interaction between its mechanical and electrical properties (cf. Ikeda [3]). In this paper, we analyse the actuator effect of a piezoelectric plate model, for different clamped boundary conditions, and subjected to the location's influence of the applied electric potentials. This is an integer optimization problem, that we numerically solve by genetic algorithms. The plate model adopted in this paper, was deduced in Figueiredo and Leal [1], by the asympotic expansion method, for nonhomogeneous and anisotropic plates, and it is a generalization of the model obtained by Sene [4] for homogeneous and isotropic plates. After this brief introduction, the rest of the paper is structured as follows. In section 2, the asymptotic piezoelectric plate model is described. Then, we present in section 3, the model's finite element discretization, as well as, the optimization problems. In the last two sections we report the numerical results for the case of a transversely isotropic plate, with constant piezoelectric and dielectric coefficients, and point out the conclusions and future work.

Received April 18, 2005.

2. The asymptotic piezoelectric plate model

In this section we first introduce some notation, concerning the geometry, the material, the loadings and boundary conditions imposed on the plate. Then, we recall the static three-dimensional piezoelectric model, for a non-homogeneous anisotropic thin plate, and, afterwards, the variational formulation of the asymptotic piezoelectric plate model, deduced by Figueiredo and Leal [1], is described.

Geometry and general notations. Let $OX_1X_2X_3$ be a fixed three-dimensional coordinate system, and $\omega \subset I\!R^2$ be a bounded domain with a Lipschitz continuous boundary $\partial\omega$ and γ_0, γ_e subsets of $\partial\omega$, such that, $\gamma_0 \neq \emptyset \neq \gamma_e$. We also define $\gamma_1 = \partial\omega \setminus \gamma_0$, $\gamma_s = \partial\omega \setminus \gamma_e$.

We consider the sets

$$\Omega = \omega \times (-h,h), \quad \Gamma_\pm = \omega \times \{\pm h\}, \quad \Gamma_D = \gamma_0 \times (-h,h), \quad \Gamma_1 = \gamma_1 \times (-h,h),$$
$$\Gamma_N = \Gamma_1 \bigcup \Gamma_\pm, \quad \Gamma_{eN} = \gamma_s \times (-h,h), \quad \Gamma_{eD} = \Gamma_\pm \bigcup \big(\gamma_e \times (-h,h)\big), \tag{1}$$

where $\overline{\Omega}$ (that is, Ω and its boundary) represents a thin plate with middle surface ω and thickness $2h$, with $h > 0$ a small constant, Γ_+ and Γ_- are, respectively, the upper and lower faces of Ω, the sets Γ_D, Γ_1 and Γ_{eN} are portions of the lateral surface $\partial\omega \times (-h,h)$ of Ω, and finally Γ_N and Γ_{eD} are portions of the boundary $\partial\Omega$ of Ω. An arbitrary point of Ω is denoted by $x = (x_1,x_2,x_3)$, where the first two components $(x_1,x_2) \in \omega$ and $x_3 \in (-h,h)$.

We denote by $\nu = (\nu_1,\nu_2,\nu_3)$ the outward unit normal vector to $\partial\Omega$. Throughout the paper, the latin indices i, j, k, l... belong to the set $\{1,2,3\}$, the greek indices α, β, μ... vary in the set $\{1,2\}$ and the summation convention with respect to repeated indices is employed, that is, $a_ib_i = \sum_{i=1}^3 a_ib_i$. Moreover we denote by $a \cdot b = a_ib_i$ the inner product of the vectors $a = (a_i)$ and $b = (b_i)$, by $Ce = (C_{ijkl}e_{kl})$ the contraction of a fourth order tensor $C = (C_{ijkl})$ with a second order tensor $e = (e_{kl})$ and by $Ce : d = C_{ijkl}e_{kl}d_{ij}$ the inner product of the tensors Ce and $d = (d_{ij})$. Given a function $\theta(x)$ defined in Ω we denote by $\theta_{,i}$ or $\partial_i\theta$ its partial derivative with respect to x_i, that is, $\theta_{,i} = \partial_i\theta = \frac{\partial\theta}{\partial x_i}$, and by $\theta_{,ij}$ or $\partial_{ij}\theta$ its second partial derivative with respect to x_i and x_j, that is, $\theta_{,ij} = \partial_{ij}\theta = \frac{\partial^2\theta}{\partial x_i \partial x_j}$. We also denote by $\frac{\partial\theta}{\partial\nu} = \nu_\alpha\partial_\alpha\theta$ the outer normal derivative of the scalar function θ along $\partial\omega$.

Material. We suppose that a piezoelectric material occupies the bounded thin plate $\overline{\Omega} \subset I\!R^3$. We denote by $C = (C_{ijkl})$, $P = (P_{ijk})$ and $\varepsilon = (\varepsilon_{ij})$, respectively, the elastic (fourth-order) tensor field, the piezoelectric (third-order) tensor field, and the dielectric (second-order) tensor field, that characterize the material. The coefficients C_{ijkl}, P_{ijk}, ε_{ij} are smooth enough functions defined in $\bar{\omega} \times [-h, h]$, and that verify the following symmetric properties: $P_{ijk} = P_{ikj}$, $\varepsilon_{ij} = \varepsilon_{ji}$, $C_{ijkl} = C_{jikl} = C_{klij}$. In addition, we impose that $C_{\alpha\beta\gamma 3} = 0 = C_{\alpha 333}$, meaning the material is monoclinic in the plane OX_1X_2, and therefore the number of independent elastic coefficients C_{ijkl} is equal to 13. We also need to introduce the reduced elastic coefficients

$$A_{\alpha\beta\gamma\rho} = C_{\alpha\beta\gamma\rho} - \frac{C_{\alpha\beta 33}C_{33\gamma\rho}}{C_{3333}}, \tag{2}$$

the modified piezoelectric coefficients $p_{3\alpha\beta}$ and corresponding vector p_3

$$p_{3\alpha\beta} = P_{3\alpha\beta} - \frac{C_{\alpha\beta 33}}{C_{3333}}P_{333}, \qquad p_3 = [p_{311} \;\; p_{322} \;\; p_{312}], \tag{3}$$

and the scalar field p_{33}

$$\begin{cases} p_{33} = \varepsilon_{33} + \dfrac{P_{333}P_{333}}{C_{3333}} \\ +\dfrac{1}{det\begin{bmatrix} C_{1313} & C_{1323} \\ C_{2313} & C_{2323}\end{bmatrix}}\begin{bmatrix} P_{323} \\ -P_{313}\end{bmatrix}^T \begin{bmatrix} C_{1313} & C_{1323} \\ C_{2313} & C_{2323}\end{bmatrix}\begin{bmatrix} P_{323} \\ -P_{313}\end{bmatrix}. \end{cases} \tag{4}$$

Finally, we also define the following matrices A and p, associated to the reduced elastic coefficients $A_{\alpha\beta\gamma\rho}$ and to the modified piezoelectric coefficients $p_{3\alpha\beta}$ and p_{33}

$$A = \begin{bmatrix} A_{1111} & A_{1122} & A_{1112} \\ A_{2211} & A_{2222} & A_{2212} \\ A_{1211} & A_{1222} & A_{1212} \end{bmatrix}, \qquad p = \tfrac{1}{p_{33}}\begin{bmatrix} p_{311}p_{311} & p_{311}p_{322} & p_{311}p_{312} \\ p_{322}p_{311} & p_{322}p_{322} & p_{322}p_{312} \\ p_{312}p_{311} & p_{312}p_{322} & p_{312}p_{312} \end{bmatrix}. \tag{5}$$

Loadings and boundary conditions. Let $f = (f_i) : \Omega \to I\!R^3$ be the density of the applied body forces acting on the plate $\overline{\Omega}$, $g = (g_i) : \Gamma_N \to I\!R^3$ the density of the applied surface forces on Γ_N ($g = 0$ in Γ_1, and g^+ and g^- are the restriction of g to Γ_+ and Γ_-, respectively). The plate is clamped along Γ_D, the electric potential applied on Γ_{eD} is represented by φ_0, and φ_0^+ and φ_0^- denote the restrictions of φ_0 to Γ_+ and Γ_-, respectively. Moreover, there is no electric loading in Ω (this means that the material is dielectric) nor on Γ_{eN}.

The three-dimensional piezoelectric plate model. In the framework of small deformations and linear piezoelectricity, the three-dimensional static equations for the piezoelectric plate are the following: *find a displacement vector field* $u : \Omega \rightarrow I\!R^3$ *and an electric potencial* $\varphi : \Omega \rightarrow I\!R^3$*, such that*

$$\sigma = Ce(u) - PE(\varphi), \quad \text{in} \quad \Omega, \tag{6}$$
$$D = Pe(u) + \varepsilon E(\varphi), \quad \text{in} \quad \Omega, \tag{7}$$
$$div\sigma = -f, \quad \text{in} \quad \Omega, \tag{8}$$
$$divD = 0\ , \quad \text{in} \quad \Omega, \tag{9}$$
$$u = 0, \quad \text{on} \quad \Gamma_D, \qquad \sigma\,\nu = g, \quad \text{on} \quad \Gamma_N, \tag{10}$$
$$D\nu = 0, \quad \text{on} \quad \Gamma_{eN}, \qquad \varphi = \varphi_0, \quad \text{on} \quad \Gamma_{eD}. \tag{11}$$

In (6-11), $\sigma : \Omega \rightarrow I\!R^9$ is the stress tensor field, $D : \Omega \rightarrow I\!R^3$ is the electric displacement vector field, $e(u)$ is the linear strain tensor, defined by

$$e(u) = \big(e_{ij}(u)\big), \qquad e_{ij}(u) = \frac{1}{2}\big(\partial_i u_j + \partial_j u_i\big), \tag{12}$$

and $E(\varphi)$ is the electric vector field, defined by

$$E(\varphi) = \big(E_i(\varphi)\big), \qquad E_i(\varphi) = -\partial_i \varphi. \tag{13}$$

The equations (6-7) are the constitutive equations, (8) is the equilibrium mechanical equation, (9) is the Maxwell-Gauss equation, (10) are the displacement and traction boundary conditions and finally (11) represents the electric boundary conditions.

The space of admissible displacements. This is a Kirchhoff-Love displacement space V_{KL} (that includes boundary conditons) defined by

$$\begin{aligned} V_{KL} = \Big\{ \;& v : \Omega \rightarrow I\!R^3, \quad v(x) = (v_1(x), v_2(x), v_3(x)), \quad x = (x_1, x_2, x_3) \in \bar{\Omega}, \\ & v_1(x) = \eta_1(x_1, x_2) - x_3 \partial_1 \eta_3(x_1, x_2), \\ & v_2(x) = \eta_2(x_1, x_2) - x_3 \partial_2 \eta_3(x_1, x_2), \\ & v_3(x) = \eta_3(x_1, x_2), \quad \text{where} \quad \eta = (\eta_i) : \omega \rightarrow I\!R^3, \\ & \eta = (\eta_1, \eta_2, \eta_3) = (0,0,0) \quad \text{and} \quad \partial_\nu \eta_3 = 0, \quad \text{in} \quad \gamma_0 \quad \Big\}. \end{aligned} \tag{14}$$

The asymptotic piezoelectric plate model. This model, derived by Figueiredo and Leal [1], by the asymptotic expansion method, is described by the following formulas (15-19). Briefly it consists of two parts. The first part **(i)** establishes that the displacement of the plate is a Kirchhoff-Love displacement, and the solution of an equation formulated in the middle plane of the plate, and the second part **(ii)** defines the exact expression of the electric potential of the plate (it is a second order polynomial with respect to the thickness variable, with coefficients that depend on the transverse component of the Kirchhoff-Love displacement).

(i): The displacement $u : \Omega \to I\!R^3$ of the plate is a Kirchhoff-Love displacement vector field, that is, $u \in V_{KL}$, with

$$\begin{aligned}
&u(x) = (u_1(x), u_2(x), u_3(x)), \quad x = (x_1, x_2, x_3) \in \bar{\Omega},\\
&u_1(x) = \zeta_1(x_1, x_2) - x_3 \partial_1 \zeta_3(x_1, x_2),\\
&u_2(x) = \zeta_2(x_1, x_2) - x_3 \partial_2 \zeta_3(x_1, x_2),\\
&u_3(x) = \zeta_3(x_1, x_2),\\
&\zeta = (\zeta_1, \zeta_2, \zeta_3) = (0,0,0) \quad \text{and} \quad \partial_\nu \zeta_3 = 0, \quad \text{in} \quad \gamma_0,
\end{aligned} \tag{15}$$

and u is the unique solution of the variational problem

$$\text{find} \quad u \in V_{KL} \quad \text{such that:} \qquad a(u,v) = l(v), \quad \forall v \in V_{KL}, \tag{16}$$

where

$$\begin{aligned}
&l(v) = \int_\Omega f \cdot v \, d\Omega + \int_{\Gamma_N} g \cdot v \, d\Gamma_N - \int_\Omega \tfrac{\varphi_0^+ - \varphi_0^-}{2h} \, p_{3\alpha\beta} \, e_{\alpha\beta}(v) \, d\Omega,\\
&a(u,v) = \int_\omega \Big[N_{\alpha\beta} \, e_{\alpha\beta}(\eta) + M_{\alpha\beta} \, \partial_{\alpha\beta} \eta_3 \Big] \, d\omega,
\end{aligned} \tag{17}$$

with $N = (N_{\alpha\beta})$ and $M = (M_{\alpha\beta})$, the second-order tensor fields associated to the Kirchhoff-Love displacement u, defined by the following matrix formula

$$\begin{bmatrix} N_{\alpha\beta} \\ M_{\alpha\beta} \end{bmatrix} = \begin{bmatrix} \int_{-h}^{+h} A_{\alpha\beta\gamma\rho} dx_3 & -\int_{-h}^{+h} x_3 A_{\alpha\beta\gamma\rho} dx_3 \\ -\int_{-h}^{+h} x_3 A_{\alpha\beta\gamma\rho} dx_3 & \int_{-h}^{+h} (x_3)^2 \big(A_{\alpha\beta\gamma\rho} + \frac{p_{3\alpha\beta} p_{3\gamma\rho}}{p_{33}} \big) dx_3 \end{bmatrix} \begin{bmatrix} e_{\gamma\rho}(\zeta) \\ \partial_{\gamma\rho} \zeta_3 \end{bmatrix}. \tag{18}$$

(ii): The electric potential φ is a second order polynomial in x_3, whose coefficients depend on ζ_3, and the exact analytic form of φ is the following

$$\varphi(x_1,x_2,x_3)=\frac{\varphi_0^+ + \varphi_0^-}{2}+h^2\,\frac{p_{3\alpha\beta}}{2p_{33}}\partial_{\alpha\beta}\zeta_3+\frac{\varphi_0^+ - \varphi_0^-}{2h}x_3-\frac{p_{3\alpha\beta}}{2p_{33}}\partial_{\alpha\beta}\zeta_3(x_3)^2. \quad (19)$$

We remark that in order to obtain (18)-(19) it must be assumed that $p_{3\alpha\beta}$ and p_{33} are independent of x_3.

3. Discrete model

We describe in this section, the approximation of (16) and (19), by the finite element method. Beginning with the matrix formulation of the bilinear form defined in (17), we proceed with the application of the finite element method to the variational formulation (16). The discrete model is completely defined in theorem 3.1. Afterwards, we formulate the integer optimization problems and briefly mention the genetic algorithms that are used to determine the solution of the numerical examples, described in section 4.

Matrix formulation of the bilinear form. We remark that the bilinear form $a(.,.)$ in (17) can be written

$$a(u,v)=\int_\omega V^T\,B\,U\,d\omega, \quad (20)$$

where, for any u and v in the space V_{KL}

$$\begin{aligned} V^T &= [e_{11}(\eta) \quad e_{22}(\eta) \quad 2e_{12}(\eta) \quad \partial_{11}\eta_3 \quad \partial_{22}\eta_3 \quad 2\partial_{12}\eta_3],\\ U^T &= [e_{11}(\xi) \quad e_{22}(\xi) \quad 2e_{12}(\xi) \quad \partial_{11}\xi_3 \quad \partial_{22}\xi_3 \quad 2\partial_{12}\xi_3], \end{aligned} \quad (21)$$

and B is the following matrix of order six

$$B=\begin{bmatrix} G & -H\\ -H & I\end{bmatrix}_{6\times 6} \quad (22)$$

where

$$G=\int_{-h}^{+h}A\,dx_3=\begin{bmatrix} \int_{-h}^{+h}A_{1111}dx_3 & \int_{-h}^{+h}A_{1122}dx_3 & \int_{-h}^{+h}A_{1112}dx_3\\ \int_{-h}^{+h}A_{2211}dx_3 & \int_{-h}^{+h}A_{2222}dx_3 & \int_{-h}^{+h}A_{2212}dx_3\\ \int_{-h}^{+h}A_{1211}dx_3 & \int_{-h}^{+h}A_{1222}dx_3 & \int_{-h}^{+h}A_{1212}dx_3 \end{bmatrix}, \quad (23)$$

and

$$H=\int_{-h}^{+h}x_3\,A\,dx_3, \qquad I=\int_{-h}^{+h}x_3\,[A+p]\,dx_3. \quad (24)$$

Finite element discretization. A rectangular domain ω is assumed and it is partitioned into a mesh of $m = n_1 n_2$ sub-rectangles, where n_1 is the number of sub-intervals in the x_1 direction and n_2 the number of sub-intervals in the x_2 direction. This means that $\omega = \bigcup_{e=1}^{m} \omega^e$, and, for each e, $\omega^e = [a_1^e, b_1^e] \times [c_2^e, d_2^e]$. The amplitudes of the real sub-intervals, $[a_1^e, b_1^e]$ and $[c_2^e, d_2^e]$, are denoted by $h_1^e = b_1^e - a_1^e$ and $h_2^e = d_2^e - c_2^e$, respectively. Moreover we suppose that the mesh $\{\omega^e\}_{e=1,\dots,m}$ is affine equivalent to the reference element $\hat{\omega} = (-1,+1) \times (-1,+1)$. The affine transformations are defined by the mappings

$$T^e : \begin{array}{lcl} \omega^e = [a_1^e, b_1^e] \times [c_2^e, d_2^e] & \longrightarrow & \hat{\omega} = (-1,+1) \times (-1,+1) \\ (x_1, x_2) & \longrightarrow & \left(\frac{2}{h_1^e}(x_1 - x_c^e), \frac{2}{h_2^e}(x_2 - y_c^e)\right), \end{array} \tag{25}$$

where x_c^e, y_c^e are the middle points of $[a_1^e, b_1^e]$ and $[c_2^e, d_2^e]$, respectively, and (x_1, x_2) is a generic element of ω^e.

The rectangular Melosh finite element (cf. subroutine planre of CALFEM [2] and Ciarlet [5]) is considered to approximate the tangential displacement field (ζ_1, ζ_2) of the Kirchhoff-Love displacement u defined in (15); the 8 degrees of freedom of the Melosh element are the values of (ζ_1, ζ_2) at each vertex of the element ω^e. The four shape functions of the Melosh finite element, defined in $\hat{\omega}$, are denoted by M_1, M_2, M_3, M_4 (the lower subscript indicates the number of the vertex). In the sequel we use also the matrix M of order 2×8, defined by

$$M = \begin{bmatrix} M_1 & 0 & M_2 & 0 & M_3 & 0 & M_4 & 0 \\ 0 & M_1 & 0 & M_2 & 0 & M_3 & 0 & M_4 \end{bmatrix}_{2\times 8}. \tag{26}$$

The Adini finite element (cf. subroutine platre of CALFEM [2] and Ciarlet [5]) is used for the approximation of the transverse displacement $u_3 = \zeta_3$; the 12 degrees of freedom characterizing this element are the values of u_3, $u_{3,1}$ and $u_{3,2}$ at each vertex of ω^e. The twelve shape functions associated to the Adini finite element, defined in $\hat{\omega}$, are denoted by N_1^j, N_2^j, N_3^j, N_4^j, with $j = 1,2,3$ (the lower subscript indicates the number of the vertex and the upper subscript j refers to the order of derivation). In the sequel, we also need to introduce the following vector N^e, associated to ω^e and to the twelve shape functions of the Adini finite element

$$N^e = \begin{bmatrix} N_1^e & N_2^e & N_3^e & N_4^e \end{bmatrix}_{1\times 12}, \quad N_i^e = \begin{bmatrix} N_i^1 & \dfrac{h_1^e}{2} N_i^2 & \dfrac{h_2^e}{2} N_i^3 \end{bmatrix}_{1\times 3}, \quad i = 1,2,3,4. \tag{27}$$

For any Kirchhoff-Love displacement u, the tangential displacements (ζ_1, ζ_2) and the transverse displacement $u_3 = \zeta_3$ are approximated, at each finite element ω^e, by the following sums

$$\begin{aligned} (\zeta_1, \zeta_2)_{|\omega^e}(x_1, x_2) &\simeq \sum_{i=1}^{4} \Big(u^e_{1i} M_i \circ T^e(x_1, x_2), u^e_{2i} M_i \circ T^e(x_1, x_2) \Big), \\ u_3 = \zeta_{3|\omega^e}(x_1, x_2) &\simeq \sum_{i=1}^{4} \big(z^e_i N^1_i + z^e_{1i} \frac{h^e_1}{2} N^2_i + z^e_{2i} \frac{h^e_2}{2} N^3_i \big) \circ T^e(x_1, x_2), \end{aligned} \tag{28}$$

where the coefficients u^e_{1i}, u^e_{2i} and z^e_i, z^e_{1i}, z^e_{2i} are the approximated values of ζ_1, ζ_2 and ζ_3, $\zeta_{3,1}$, $\zeta_{3,2}$, respectively, at node i of ω^e. Moreover, we denote by u^e_{tg} and u^e_{tv}, the vectors with eight and twelve components, respectively, that approximate, in ω^e, the tangential and transverse displacements (ζ_1, ζ_2) and $u_3 = \zeta_3$, that is,

$$\begin{aligned} u^e_{tg} &= [(u^e_{1i}, u^e_{2i})_{i=1} \;\; (u^e_{1i}, u^e_{2i})_{i=2} \;\; (u^e_{1i}, u^e_{2i})_{i=3} \;\; (u^e_{1i}, u^e_{2i})_{i=4}]^T \simeq (\zeta_1, \zeta_2)_{|\omega^e} \\ u^e_{tv} &= [(z^e_i, z^e_{1i}, z^e_{2i})_{i=1,2,3,4}]^T \simeq \zeta_{3|\omega^e}. \end{aligned} \tag{29}$$

In addition, the following vector, with 20 components, is introduced

$$u^e = \begin{bmatrix} u^e_{tg} \\ u^e_{tv} \end{bmatrix}_{20\times 1}, \tag{30}$$

that is the local finite element approximation of the displacement vector field $(\zeta_1, \zeta_2, \zeta_3)$ in ω^e.

In order to describe the discrete problem, corresponding to (16) and (19), some further notation must be detailed, concerning the numeration of the global degrees of freedom and nodes in the mesh. So, let n be the number of global nodes of the mesh, and

$$u_{tv} = [u^e_{tv}]^m_{e=1} \in I\!R^{3n}, \quad \text{and} \quad u_{tg} = [u^e_{tg}]^m_{e=1} \in I\!R^{2n}, \tag{31}$$

be the global approximations of the transverse and tangential displacements (ζ_3 and (ζ_1, ζ_2), respectively), and let

$$u = [u_{tg} \; u_{tv}] \in I\!R^{2n+3n}, \quad u_{tg} = (u_{1j}, u_{2j})^n_{j=1}, \quad u_{tv} = (z_j, z_{1j}, z_{2j})^n_{j=1} \tag{32}$$

be the global approximation of $(\zeta_1, \zeta_2, \zeta_3)$ in ω. Moreover, the following subsets of indices are defined

$$\begin{array}{ll} L_1,\; L_2, & L_1 \cup L_2 \subset \{1, 2, ..., 2n\}, \\ J_1,\; J_2,\; J_3, & J_1 \cup J_2 \cup J_3 \subset \{2n+1, ..., 5n\}. \end{array} \tag{33}$$

The two sets of indices L_1 and L_2 represent the number of the global degrees of freedom, that are attached to the values of the tangential displacements ζ_1 and ζ_2, respectively, at the boundary nodes of the mesh, where the plate is clamped. Analogously, the three sets J_k, for $k = 1, 2, 3$, represent the number of the global degrees of freedom, associated to the transverse displacement $u_3 = \zeta_3$ at the boundary nodes of the mesh, where the plate is clamped: the subscript $k = 1$ refers to the displacement, $k = 2$ to the first derivative of the displacement with respect to x_1, and $k = 3$ to the first derivative of the displacement with respect to x_2. If S is a set of indices, and $u_{tv} \in I\!R^{3n}$, $u_{tg} \in I\!R^{2n}$, we denote by $u_{tv\,S}$, $u_{tg\,S}$ the sub-vectors of u_{tv} and u_{tg} respectively, whose components have the indices in S.

Discrete model. Based on the choice of the finite elements described before and using the notations introduced in (33), the following result is obtained.

Theorem 3.1. *The discrete problem associated to (16) takes the following form:*

$$\begin{cases} \textit{Find} \quad u = [u_{tg} \;\; u_{tv}] \in I\!R^{5n} \quad \textit{such that}: \\ u_{tg\,L_1} = u_{tg\,L_2} = 0, \qquad u_{tv\,J_1} = u_{tv\,J_2} = u_{tv\,J_3} = 0, \\ Ku = F. \end{cases} \tag{34}$$

At the element level, the square matrix K and the vector F are defined respectively, by K^e in (40) and F^e in (44). Furthermore, the finite element approximation of the electric potential (19) is defined by

$$\varphi(x_1, x_2, x_3)_{|\omega^e \times (-h,+h)} \simeq \frac{\varphi_0^+ + \varphi_0^-}{2} + \frac{\varphi_0^+ - \varphi_0^-}{2h} x_3 + \frac{1}{2p_{33}} \, [h^2 - x_3^2] \; p_3 \, S^e u_{tv}^e, \tag{35}$$

where S^e, defined in (39), is the matrix of the second derivatives of the Adini's finite element shape functions.

Proof: The discretisation of (16) can be obtained, directly, by replacing in (20) $(\zeta_1, \zeta_2, \zeta_3)$ and (η_1, η_2, η_3) by the approximations defined in (28). In fact, for any u and v in V_{KL}

$$a(u, v) = \sum_{e=1}^{m} \int_{\omega^e} V^T \, B \, U \, d\omega^e = \sum_{e=1}^{m} \frac{h_1^e h_2^e}{4} \int_{\hat{\omega}} V^T \, B \, U \, d\hat{\omega}, \tag{36}$$

and due to (28), at each finite element $\omega^e = T^e(\hat{\omega})$, we can use the approximations

$$V \simeq \begin{bmatrix} L^e v_{tg}^e \\ S^e v_{tv}^e \end{bmatrix}, \qquad U \simeq \begin{bmatrix} L^e u_{tg}^e \\ S^e u_{tv}^e \end{bmatrix}, \tag{37}$$

where L^e and S^e are two matrices, that depend on the derivatives of the shape functions of the Melosh and Adini's finite elements, respectively. The matrix L^e has order 3×8 and is defined by

$$L^e = [L_1^e\ L_2^e\ L_3^e\ L_4^e]_{3\times 8}, \quad L_i^e = \begin{bmatrix} \frac{2}{h_1^e} M_{i,1} & 0 \\ 0 & \frac{2}{h_2^e} M_{i,2} \\ \frac{2}{h_2^e} M_{i,2} & \frac{2}{h_1^e} M_{i,1} \end{bmatrix}_{3\times 2} \quad i = 1, 2, 3, 4, \tag{38}$$

and S^e is a matrix of order 3×12 defined by

$$S^e = [S_1^e\ S_2^e\ S_3^e\ S_4^e]_{3\times 12}, \quad S_i^e = \begin{bmatrix} \frac{4}{h_1^e h_1^e} \big(N_{i,11}^1 & \frac{h_1^e}{2} N_{i,11}^2 & \frac{h_2^e}{2} N_{i,11}^3 \big) \\ \frac{4}{h_2^e h_2^e} \big(N_{i,22}^1 & \frac{h_1^e}{2} N_{i,22}^2 & \frac{h_2^e}{2} N_{i,22}^3 \big) \\ \frac{2\times 4}{h_1^e h_2^e} \big(N_{i,12}^1 & \frac{h_1^e}{2} N_{i,12}^2 & \frac{h_2^e}{2} N_{i,12}^3 \big) \end{bmatrix}_{3\times 3} \quad i = 1, 2, 3, 4. \tag{39}$$

Now introducing (37) and (38-39) in (36) we get immediately

$$\begin{aligned} a(u,v) &\simeq \sum_{e=1}^{m} \frac{h_1^e h_2^e}{4} \int_{\hat{\omega}} \left(\begin{bmatrix} L^e v_{tg}^e \\ S^e v_{tv}^e \end{bmatrix}^T B \begin{bmatrix} L^e u_{tg}^e \\ S^e u_{tv}^e \end{bmatrix} \right) d\omega^e \\ &= \sum_{e=1}^{m} v^{eT} \underbrace{\frac{h_1^e h_2^e}{4} \int_{\hat{\omega}} \left(\begin{bmatrix} L^{eT} & 0 \\ 0 & S^{eT} \end{bmatrix}_{20\times 6} B_{6\times 6} \begin{bmatrix} L^e & 0 \\ 0 & S^e \end{bmatrix}_{6\times 20} \right) d\omega^e}_{K^e}\, u^e \\ &= \sum_{e=1}^{m} v^{eT} K^e u^e. \end{aligned} \tag{40}$$

On the other hand, the linear form $l(v)$ in (17) can be written

$$
\begin{aligned}
l(v) &= \int_\Omega f\cdot v\,d\Omega + \int_{\Gamma_N} g\cdot v\,d\Gamma_N - \int_\Omega \frac{\varphi_0^+-\varphi_0^-}{2h}\,p_{3\alpha\beta}\,e_{\alpha\beta}(v)\,d\Omega \\
&= \sum_{e=1}^m \frac{h_1^e h_2^e}{4}\Big[\int_{\hat\omega} \underbrace{\Big(\int_{-h}^{+h} f_\alpha\,dx_3 + g_\alpha^+ + g_\alpha^-\Big)}_{F_\alpha}(\eta_\alpha - x_3\partial_\alpha\eta_3)\,d\hat\omega \\
&+ \int_{\hat\omega} \underbrace{\Big(\int_{-h}^{+h} f_3\,dx_3 + g_3^+ + g_3^-\Big)}_{F_3} v_3\,d\hat\omega + \int_{\hat\omega}\frac{\varphi_0^+-\varphi_0^-}{2h}\Big(\int_{-h}^{+h} p_{3\alpha\beta}\,e_{\alpha\beta}(v)\,dx_3\Big)\,d\hat\omega\Big].
\end{aligned}
\tag{41}
$$

But for any v in V_{KL}, $p_{3\alpha\beta}\,e_{\alpha\beta}(v) = p_{3\alpha\beta}[e_{\alpha\beta}(\eta) - x_3\partial_{\alpha\beta}\eta_3]$, and due to (28), the following approximations can be used, in each finite element $\omega^e = T^e(\hat\omega)$,

$$
\begin{aligned}
(\eta_1,\eta_2) &\simeq M v_{tg}^e, \\
v_3 = \eta_3 &\simeq N^e v_{tv}^e,
\end{aligned}
\qquad p_{3\alpha\beta}\,e_{\alpha\beta}(v) \simeq p_3\,[L^e v_{tg}^e - x_3 S^e v_{tv}^e]_{3\times 1}. \tag{42}
$$

So, denoting

$$
f_{tg} = [F_1\ \ F_2]^T \quad \text{and} \quad f_{tv} = [F_3] \tag{43}
$$

and assuming, to simplify the following computations, that f_α, g_α^+ and g_α^- are independent of $x_3 \in (-h,h)$, we obtain that $l(v)$ is approximated by

$$
\begin{aligned}
l(v) \simeq \sum_{e=1}^m \Big[(v_{tg}^e)^T\, &\underbrace{\frac{h_1^e h_2^e}{4}\int_{\hat\omega} M^T f_{tg} - \frac{\varphi_0^+-\varphi_0^-}{2h}\Big(\int_{-h}^{+h} L^{eT}\,p_3^T\,dx_3\Big)}_{F_{tg}^e} \\
+ (v_{tv}^e)^T\, &\underbrace{\frac{h_1^e h_2^e}{4}\int_{\hat\omega} N^{eT} f_{tv} + \frac{\varphi_0^+-\varphi_0^-}{2h}\Big(\int_{-h}^{+h} x_3\,S^{eT}\,p_3^T\,dx_3\Big)}_{F_{tv}^e}\Big]\,d\hat\omega = \sum_{e=1}^m v^{eT} F^e,
\end{aligned}
\tag{44}
$$

where $F^e = \begin{bmatrix} F_{tg}^e \\ F_{tv}^e \end{bmatrix}$ is a vector with 20 components. Therefore, from (40) and (44), we conclude that the asymptotic variational model (16) is approximated by the linear equation

$$\sum_{e=1}^{m} v^{eT} K^e u^e = \sum_{e=1}^{m} v^{eT} F^e, \tag{45}$$

which consequently implies the equation $Ku = F$ in (34). The matrix K, of order $5n$, and the vector F, also of order $5n$, are obtained by assembling the element matrices K^e and vectors F^e, by the usual finite element procedure. The components of the unknown u have the form described (31-32).

Finally, to obtain (35) it is enough to use (19) and to remark that, in each finite element $\omega^e = T^e(\hat{\omega})$, we can use the following approximation

$$p_{3\alpha\beta}\, \partial_{\alpha\beta}(\zeta_3)_{|\omega^e} \simeq p_3\, S^e u^e_{tv}. \quad \square \tag{46}$$

Optimization problems. We describe now the integer optimization problems, that model the actuator effect of the discrete piezoelectric anisotropic plate, as a function of the position of a fixed number of electrodes, through which the electric potential is applied. The electrodes are stuck on some parts or on the whole upper or/and lower faces of the plate, and they are considered very thin and very light, such that, their mechanical properties are neglected. In addition we suppose the area occupied by each electrode is the area of one finite element of the mesh $\omega = \bigcup_{e=1}^{m} \omega^e$, and at each electrode the applied electric potential is equal to φ_0^+, if the electrode is on the top of the plate, and to φ_0^-, if the electrode is on the bottom.

Let us introduce, for a mesh with m finite elements, the new integer variables $y_i = (i, pe)$, $i = 1, ..., m$, where the first component represents the total number of electrodes in the plate, and the second component pe denotes the position of the projections of these i electrodes in the mesh. Thus i is a single element of the set $Y = \{1, 2, \cdots, m\}$ and pe is a subset of Y, with i elements, that is, $\#pe = i$, where $\#$ represents the cardinal of a set. For example, for $i = 3$ and $y_3 = (3, [1, 5, 10])$, it means that, the applied electric potential φ_0^- and φ_0^+ are zero everywhere on the mesh $\omega = \bigcup_{e=1}^{m} \omega^e$, except at the finite elements 1, 5, 10, where these two applied electric potential can not be simultaneously zero, and:

- if $\varphi_0^- = 0$ (respectively $\varphi_0^+ = 0$), at the finite elements 1, 5, 10, then, there are 3 electrodes located at the upper face (respectively, lower face) of the plate, and whose projections on the middle plane of the plate are the finite elements 1, 5, 10,

- if both $\varphi_0^- \neq 0 \neq \varphi_0^+$ at the finite elements 1, 5, 10, there is a total of 2×3 electrodes on the plate, 3 at the top and 3 at the bottom, whose projections, on the middle plane of the plate, are the finite elements 1, 5, 10.

Then, for each $i = 1, ..., m$, the optimization problems that we address in this paper are the following:

$$\left[\begin{array}{l} \max\limits_{y_i} d_i(y_i) = \max\limits_{y_i} \Big(\max\limits_{j=1,\dots,n} \|(u_{1j}, u_{2j}, z_j)\|_{I\!R^3} \Big), \\ \text{subject to :} \left[\begin{array}{l} y_i = (i, pe), \quad pe \in C_i^m(Y), \quad \#pe = i, \\ \left\{\begin{array}{l} \text{Find} \quad u = [u_{tg} \;\; u_{tv}] \in I\!R^{5n} \quad \text{such that :} \\ u_{tg_{L_1}} = u_{tg_{L_2}} = 0, \qquad u_{tv\,J_1} = u_{tv\,J_2} = u_{tv\,J_3} = 0, \\ Ku = F, \end{array}\right. \end{array}\right. \end{array}\right. \tag{47}$$

where the triple (u_{1j}, u_{2j}, z_j) (cf.(32)) is the approximation of $(\zeta_1, \zeta_2, \zeta_3)$ at the global node j, $\|.\|_{I\!R^3}$ is the usual Euclidean norm in $I\!R^3$, the objective function $d_i(y_i)$ is the node's maximum displacement, for the case where there are i electrodes, whose projections are located at the positions pe defined in y_i, and, finally, $C_i^m(Y)$ represents the set of subsets of Y, with i distinct elements. It should be pointed out that F depends on y_i, cf. (44), therefore for each y_i, the vector u depends on y_i, and consequently (47) is an optimization problem, which has the following interpretation: given the boundary conditions and the mechanical loadings, the aim is to determine, the location pe of the i electrodes, that cause a maximum node's displacement in the plate.

It should be referred that this is a combinatorial problem, since different combinations of the positions of the electrodes can produce different displacements. In particular, the set $C_i^m(Y)$, that is the admissible set of the optimization variable pe, has cardinal equal to the combinations of m, i to i, that is, $C_i^m = \frac{m!}{i!(m-i)!}$ (for instance for a mesh with 25 finite elements and 3 electrodes, we have $C_3^{25} = 2300$).

Obviously, the solutions of these optimization problems strongly depend on the loadings and the boundary conditions imposed to the plate. In order to achieve a better understanding of the actuator effect, it can be assumed that all the mechanical loadings $f = (f_i)$ and $g = (g_i)$ are zero. To analyze the influence of the clamped boundary conditions, it may be considered that the plate is clamped on different parts of the lateral surface (this means that we vary the definition of the set $\gamma_0 \subset \partial\omega$).

The problem (47) is a single optimization problem, since there is only one objective, and the purpose is to determine the global optimum solution. Nevertheless, we are interested in finding the optimum location of the electrodes, as well as, the optimum number of these electrodes. Two objectives can thus be considered: the maximization of the displacements of any of the nodes of the mesh and the minimization of the number of electrodes. This corresponds to the following multi-objective problem (associated to (47))

$$\left[\begin{array}{ll} \max\limits_{y_i} d_i(y_i) \quad \wedge \quad \min i & \\ \text{subject to :} & \left[\begin{array}{l} y_i = (i, pe), \quad pe \in C_i^m(Y), \quad \#pe = i, \quad i = 1, 2, ..., m, \\ \begin{cases} \text{Find} \quad u = [u_{tg} \;\; u_{tv}] \in I\!R^{5n} \quad \text{such that :} \\ u_{tg\,L_1} = u_{tg\,L_2} = 0, \qquad u_{tv\,J_1} = u_{tv\,J_2} = u_{tv\,J_3} = 0, \\ Ku = F, \end{cases} \end{array}\right. \end{array}\right. \tag{48}$$

where m is the total number of finite elements in the mesh. For this last problem the aim is to characterize, not the optimum solution, but a set of optimal solutions, the so-called set of Pareto optimal solutions; these are solutions that can not improve the performance of one objective, without making worse the performance of the other.

Genetic Algorithms. Solving multi-objective (engineering) problems is a very difficult task since, in general, the objectives conflict across a high-dimensional problem space. Genetic algorithms (GAs) (cf. Goldberg [6]) are particularly suited to tackle this class of problems because they work with populations of candidate solutions, and use some diversity-preserving mechanisms, that enable to find, in a single run, widely different multiple potential Pareto-optimal solutions (cf. Deb [7]).

The Elitist GA, described in Costa and Oliveira [8] and Costa et al. [9], was applied to problems (47) and (48), with standard values for the parameters. We briefly describe next some technical features and the parameters of this GA.

The optimization variables $y_i = (i, pe)$ in problem (48) were encoded using binary strings, referred as chromosomes. For example, consider a fixed mesh with m finite elements and n nodes: a binary string represents the sequence of the m finite elements in the mesh, as well as the position pe of i electrodes – 1 means that, the respective finite element is the projection of one electrode, where it has been applied an electric potential, while 0 means that, for the corresponding finite element finite, there is no electrode. To each string it is assigned a displacement u, that is the solution of the inner linear system $Ku = F$, in problem (48). We recall that u is a vector containing the displacements of all the n nodes of the mesh. The aim of the multi-objective problem (48) is the maximization of the displacement of any of the n nodes of the mesh, as a function of the projection's location of the electrodes in the mesh, as well as, the minimization of the number of electrodes.

The stopping criterion of the GA has varied according to the size m of the finite element mesh: for example for the meshes with 3x3, 4x4 and 5x5 finite elements, the maximum number of generations allowed was 30, 50 and 100, respectively, and the number of binary decision variables (the chromosomes) was, respectively, 9, 16 and 25. For all the meshes, we have used an initial population size of 100 chromosomes. A tournament selection, a two point crossover and an uniform mutation were adopted. The crossover probability was, for all the meshes, 0.7. The mutation probability was given by $1/b$ where b is the binary string length. The elitism level considered was 10. The value of sigma share (σ_{share}) was kept constant for all the meshes and equal to 1. For sharing purposes, the distance measure considered was the Hamming distance between chromosomes.

4. Numerical tests

In this section we report several experiments. For all the tests, the stiffness matrices K and force vectors F have been evaluated with the subroutines *planre* and *platre*, of the CALFEM toolbox of MATLAB [2], and, the genetic algorithms have been implemented in C^{++}.

In all the numerical tests presented in this section, we have supposed that the reduced elastic coefficients $A_{\alpha\beta\gamma\rho}$ are independent of the thickness variable x_3. This assumption clearly simplifies the linear system $Ku = F$ in the optimization problem (47). In fact, this implies that the matrix H defined in (24) is zero, and thus the element stiffness matrix K^e (40) reduces to

$$K^e = \frac{h_1^e h_2^e}{4} \int_{\hat{\omega}} \left[\begin{array}{cc} L^{eT} G L^e & 0 \\ 0 & S^{eT} I S^e \end{array} \right]_{20\times 20} d\omega^e = \left[\begin{array}{c} K_{tg}^e \\ K_{tv}^e \end{array} \right]. \qquad (49)$$

Hence, the system (45) is equivalent to the two following independent linear systems

$$\sum_{e=1}^{m} {v_{tg}^{e}}^{T} K_{tg}^{e} u_{tg}^{e} = \sum_{e=1}^{m} {v_{tg}^{e}}^{T} F_{tg}^{e} \quad \text{and} \quad \sum_{e=1}^{m} {v_{tv}^{e}}^{T} K_{tv}^{e} u_{tv}^{e} = \sum_{e=1}^{m} {v_{tv}^{e}}^{T} F_{tv}^{e}. \tag{50}$$

Let us now denote by K_{tg} and K_{tv} the square matrices of order $2n$ and $3n$, defined, at the element level, by respectively, K_{tg}^e and K_{tv}^e, and denote by F_{tg} and F_{tv} the vectors of order $2n$ and $3n$, defined, at the element level, by respectively, F_{tg}^e and F_{tv}^e. Then, from (50), we conclude that the system in (47) is equivalent to the two independent linear systems

$$\begin{cases} \text{Find} \quad u_{tg} \in I\!R^{2n} \quad \text{such that :} \\ u_{tg\,L_1} = u_{tg\,L_2} = 0, \\ K_{tg} u_{tg} = F_{tg}, \end{cases} \quad \text{and} \quad \begin{cases} \text{Find} \quad u_{tv} \in I\!R^{3n} \quad \text{such that :} \\ u_{tv\,J_1} = u_{tv\,J_2} = u_{tv\,J_3} = 0, \\ K_{tv} u_{tv} = F_{tv}, \end{cases} \tag{51}$$

whose unknowns are the tangential and transverse displacement, u_{tg} and u_{tv}, respectively. It should be added that the left system depends on φ_0^+ or/and φ_0^-, through F_{tg}, but the right system is independent of these electric potential data. Thus, the unknown u_{tg} depends on φ_0^+ or/and φ_0^-, but u_{tv} is independent of these data. The optimization problem (47) reduces to

$$\left[\begin{array}{l} \max\limits_{y_i} d_i(y_i) = \max\limits_{y_i} \big(\max\limits_{j=1,\dots,n} \|(u_{1j}, u_{2j})\|_{I\!R^2} \big), \\ \text{subject to :} \left[\begin{array}{l} y_i = (i, pe), \quad pe \in C_i^m(Y), \quad \#pe = i, \\ \begin{cases} \text{Find} \quad u_{tg} \in I\!R^{2n} \quad \text{such that :} \\ u_{tg\,L_1} = u_{tg\,L_2} = 0, \\ K_{tg} u_{tg} = F_{tg}, \end{cases} \end{array} \right. \end{array} \right. \tag{52}$$

and the right linear system in (51) can be solved independently of the optimization problem, because it is independent of the integer variable $y = (i, pe)$.

We consider now a fixed three-dimensional coordinate system $OXYZ$, and a plate $\overline{\Omega} = [0, L_1] \times [0, L_2] \times [-h, +h]$, with a rectangular middle plane $\omega = (0, L_1) \times (0, L_2)$, whose sides have length L_1, L_2, and thickness $2h$. The geometric, electric potential and mechanical loadings data, imposed to the plate, are given in Table 1. Moreover, we assume that this plate is made of a piezoelectric material, polarized through the thickness. The elastic, piezoelectric and dielectric coefficients (C_{ijkl}, P_{ijk} and ε_{ij}) are given in relations (53) and in Table 2 (these data are also used by Bernadou and Haenel [10]).

$$\begin{bmatrix} C_{1111} & C_{1122} & C_{1133} & C_{1123} & C_{1131} & C_{1112} \\ & C_{2222} & C_{2233} & C_{2223} & C_{2231} & C_{2212} \\ & & C_{3333} & C_{3323} & C_{3331} & C_{3312} \\ & & & C_{2323} & C_{2331} & C_{2312} \\ & sym. & & & C_{3131} & C_{3112} \\ & & & & & C_{1212} \end{bmatrix} = \begin{bmatrix} C_{11} & C_{12} & C_{13} & 0 & 0 & 0 \\ C_{12} & C_{11} & C_{13} & 0 & 0 & 0 \\ C_{13} & C_{13} & C_{33} & 0 & 0 & 0 \\ 0 & 0 & 0 & C_{44} & 0 & 0 \\ 0 & 0 & 0 & 0 & C_{44} & 0 \\ 0 & 0 & 0 & 0 & 0 & C_{66} \end{bmatrix}$$

$$\begin{bmatrix} P_{111} & P_{122} & P_{133} & P_{123} & P_{131} & P_{112} \\ P_{211} & P_{222} & P_{233} & P_{223} & P_{231} & P_{212} \\ P_{311} & P_{322} & P_{333} & P_{323} & P_{331} & P_{312} \end{bmatrix} = \begin{bmatrix} 0 & 0 & 0 & 0 & P_{15} & 0 \\ 0 & 0 & 0 & P_{15} & 0 & 0 \\ P_{31} & P_{31} & P_{33} & 0 & 0 & 0 \end{bmatrix} \tag{53}$$

$$\begin{bmatrix} \varepsilon_{11} & \varepsilon_{12} & \varepsilon_{13} \\ & \varepsilon_{22} & \varepsilon_{23} \\ sym. & & \varepsilon_{33} \end{bmatrix} = \begin{bmatrix} \varepsilon_{11} & 0 & 0 \\ 0 & \varepsilon_{11} & 0 \\ 0 & 0 & \varepsilon_{33} \end{bmatrix}.$$

Parameter	Unit	Value
L_1	m	1
L_2	m	1
h	m	0.01
φ_0^+	V	-100
φ_0^-	V	0
$f = (f_i)$	N	(0,0,0)
$g = (g_i)$	N	(0,0,0)

Table 1. Geometric, electric potential and mechanical loadings data

In Tables 1-2 the unit symbols m, V, N, GPa, Cm^{-2} and Fm^{-1} mean, respectively, meter, volt, newton, giga pascal, coulomb per square meter and farad per meter. The definition (53) and Table 2 states that the chosen material is homogeneous and transversely isotropic in the plane OXY, with constant piezoelectric and dielectric coefficients.

In the sequel and for each finite element mesh of ω, the finite elements and the nodes are numbered from the left side $ls = \{0\} \times [0, L_2]$ to the right side $rs = \{L_1\} \times [0, L_2]$ and from the bottom side $bs = [0, L_1] \times \{0\}$ to the top side

Parameter	Unit	Value
C_{11}	GPa	126
C_{12}	GPa	79.5
C_{13}	GPa	84.1
C_{33}	GPa	117
C_{44}	GPa	23
C_{66}	GPa	23.25
P_{31}	Cm^{-2}	-6.5
P_{33}	Cm^{-2}	23.3
P_{15}	Cm^{-2}	17
ε_{11}	Fm^{-1}	1.503×10^{-8}
ε_{33}	Fm^{-1}	1.3×10^{-8}

TABLE 2. Elastic, piezoelectric and dielectric data

$ts = [0, L_1] \times \{L_2\}$ of ω, as explained in the Tables 3 and 4. The solutions

		ts		
	7	8	9	
ls	4	5	6	rs
	1	2	3	
		bs		

13	14	15	16
9	10	11	12
5	6	7	8
1	2	3	4

bs

21	22	23	24	25
16	17	18	19	20
11	12	13	14	15
6	7	8	9	10
1	2	3	4	5

bs

TABLE 3. Finite element's numeration of the meshes with 3x3, 4x4 and 5x5 finite elements

13	14	15	16
9	10	11	12
5	6	7	8
1	2	3	4

21	22	23	24	25
16	17	18	19	20
11	12	13	14	15
6	7	8	9	10
1	2	3	4	5

31	32	33	34	35	36
25	26	27	28	29	30
19	20	21	22	23	24
13	14	15	16	17	18
7	8	9	10	11	12
1	2	3	4	5	6

TABLE 4. Node's numeration for the meshes with 3x3, 4x4 and 5x5 finite elements

produced by the genetic algorithms are displayed in Tables 5 and 6, for two groups of clamped boundary conditions, for three different meshes of the middle plane ω (respectively with 3×3, 4×4 and 5×5 finite elements) and for 1 to 5 electrodes. In these tables, NFE is the number of finite elements of

NFE		3×3		4×4		5×5	
BC	ne	*pe*	N - mv	*pe*	N - mv	*pe*	N - mv
1	1	[1]	13 - 7.678	[1]	21 - 5.097	[1]	31 - 3.592
		[3]	16 - 7.678	[4]	25 - 5.097	[5]	36 - 3.592
	2	[1,4]	13 - 13.88	[1,9]	21 - 9.182	[1,16]	31 - 6.602
		[3,6]	16 - 13.88	[4,12]	25 - 9.182	[5,20]	36 - 6.602
	3	[1,4,7]	13 - 15.92	[1,5,9]	21 - 13.12	[1,6,16]	31 - 9.377
		[3,6,9]	16 - 15.92	[4,8,12]	25 - 13.12	[5,10,20]	36 - 9.377
	4	[1,2,4,7]	13 - 17.77	[1,2,5,9]	21 - 15.16	[1,6,11,16]	31 - 12.09
		[2,3,6,9]	16 - 17.77	[3,4,8,12]	25 - 15.16	[5,10,15,20]	36 - 12.09
	5	[1,2,4,5,7]	13 - 19.11	[1,2,5,6,9]	21 - 17.02	[1,2,6,11,16]	31 - 13.94
		[2,3,5,6,9]	16 - 19.11	[3,4,7,8,12]	25 - 17.02	[4,5,10,15,20]	36 - 13.94
2	1	[7]	14 - 4.544	[13]	22 - 3.518	[21]	32 - 2.857
		[9]	15 - 4.544	[16]	24 - 3.518	[25]	35 - 2.857
	2	[7,8]	14 - 5.677	[14,15]	23 - 4.480	[22,23]	33 - 3.669
		[8,9]	15 - 5.677			[23,24]	34 - 3.669
	3	[5,7,8]	14 - 6.783	[10,14,15]	23 - 5.403	[18,22,23]	33 - 4.429
		[5,8,9]	15 - 6.783	[11,14,15]	23 - 5.403	[18,23,24]	34 - 4.429
	4	[4,5,7,8]	14 - 7.840	[10,11,14,15]	23 - 6.321	[17,18,22,23]	33 - 5.170
		[5,6,8,9]	15 - 7.840			[18,19,22,23]	34 - 5.170
	5	[4,5,6,7,8]	14 - 8.741	[9,10,11,14,15]	23 - 7.136	[16,17,18,22,23]	33 - 5.861
		[4,5,6,8,9]	15 - 8.741	[10,11,12,14,15]	23 - 7.136	[18,19,22,23,24]	34 - 5.861

TABLE 5. Solutions *pe* and N for BC=1,2

the mesh, ne is the number of electrodes, *pe* is the position of the projections of the electrodes in the mesh, N is the number of the global node of the mesh where the maximum displacement is attained, mv represents the maximum value of the objective function (that is, if ne=i, mv is the displacement of node N, for i electrodes) in meters and multiplied by the scalar 10^6, and finally BC denotes the type of clamped boundary conditions. If BC=1, ω is clamped only in the bottom side ($\gamma_0 = bs$); if BC=2, ω is clamped in the left, bottom and right sides ($\gamma_0 = ls \cup bs \cup rs$); if BC=3, ω is clamped in the two opposite left and right sides ($\gamma_0 = ls \cup rs$); if BC=4, ω is clamped in the two consecutive bottom and right sides ($\gamma_0 = bs \cup rs$).

A direct observation of Tables 5 and 6 leads to the following conclusions. For each type of clamped boundary conditions and for each fixed number of electrodes, there is always more than one solution *pe*, except for the case BC=4 and ne=1. Moreover, these multiple solutions correspond to symmetric positions of the projections of the electrodes in the mesh. These results are physical meaningful since the middle plane w is a square and the finite element meshes are regular and square (3x3, 4x4, 5x5). The Tables 5 and

NFE		3×3		4×4		5×5	
BC	ne	*pe*	N - mv	*pe*	N - mv	*pe*	N - mv
3	1	[1]	2 - 4.506	[1]	2 - 3.503	[1]	2 - 2.852
		[3]	3 - 4.506	[4]	4 - 3.503	[5]	5 - 2.852
		[7]	14 - 4.506	[13]	22 - 3.503	[21]	32 - 2.852
		[9]	15 - 4.506	[16]	24 - 3.503	[25]	35 - 2.852
	2	[1,2]	2 - 5.579	[2,3]	3 - 4.497	[2,3]	3 - 3.697
		[2,3]	3 - 5.579	[14,15]	23 - 4.497	[3,4]	4 - 3.697
		[7,8]	14 - 5.579			[22,23]	33 - 3.697
		[8,9]	15 - 5.579			[23,24]	34 - 3.697
	3	[1,2,5]	2 - 6.459	[2,3,6]	3 - 5.297	[2,3,8]	3 - 4.405
		[2,3,5]	3 - 6.459	[2,3,7]	3 - 5.297	[3,4,8]	4 - 4.405
		[5,7,8]	14 - 6.459	[10,14,15]	23 - 5.297	[18,22,23]	33 - 4.405
		[5,8,9]	15 - 6.459	[11,14,15]	23 - 5.297	[18,23,24]	34 - 4.405
	4	[1,2,4,5]	2 - 7.296	[2,3,6,7]	3 - 6.093	[2,3,7,8]	3 - 5.089
		[2,3,5,6]	3 - 7.296	[10,11,14,15]	23 - 6.093	[3,4,8,9]	4 - 5.089
		[4,5,7,8]	14 - 7.296			[17,18,22,23]	33 - 5.089
		[5,6,8,9]	15 - 7.296			[18,19,23,24]	34 - 5.089
	5	[1,2,4,5,6]	2 - 7.956	[2,3,5,6,7]	3 - 6.814	[2,3,6,7,8]	3 - 5.737
		[2,3,4,5,6]	3 - 7.956	[2,3,6,7,8]	3 - 6.814	[3,4,8,9,10]	4 - 5.737
		[4,5,6,7,8]	3 - 7.956	[9,10,11,14,15]	23 - 6.814	[16,17,18,22,23]	33 - 5.737
		[4,5,6,8,9]	15 - 7.956	[10,11,12,14,15]	23 - 6.814	[18,19,20,23,24]	34 - 5.737
4	1	[7]	13 - 5.997	[13]	21 - 4.502	[21]	31 - 3.604
	2	[4,7]	13 - 8.870	[9,13]	21 - 6.676	[16,21]	31 - 5.344
		[7,8]	13 - 8.870	[13,14]	21 - 6.676	[21,22]	31 - 5.344
	3	[1,4,7]	13 - 12.13	[5,9,13]	21 - 8.830	[11,16,21]	31 - 7.077
		[7,8,9]	13 - 12.13	[13,14,15]	21 - 8.830	[21,22,23]	31 - 7.077
	4	[1,2,4,7]	13 - 14.15	[1,5,9,13]	21 - 10.90	[6,11,16,21]	31 - 8.520
		[6,7,8,9]	13 - 14.15	[13,14,15,16]	21 - 10.90	[21,22,23,24]	31 - 8.520
	5	[1,2,4,5,7]	13 - 15.74	[1,2,5,9,13]	21 - 12.41	[1,6,11,16,21]	31 - 9.929
		[5,6,7,8,9]	13 - 15.74	[12,13,14,15,16]	21 - 12.41	[21,22,23,24,25]	31 - 9.929

TABLE 6. Solutions *pe* and N for BC=3,4

6 also show that a refinement of the mesh clearly defines the optimal location of the projections of the electrodes (see Table 7 that also illustrates this fact); the corresponding nodes N, where the displacements are maximum, are

precisely those nodes that are far away from the clamped sides. We also conclude, that, among the four boundary conditions, the case BC=1 originates larger displacements than the other 3 cases.

7	8	9
4	5	6
1	2	3

13	14	15	16
9	10	11	12
5	6	7	8
1	2	3	4

21	22	23	24	25
16	17	18	19	20
11	12	13	14	15
6	7	8	9	10
1	2	3	4	5

TABLE 7. Optimal location of the projections of 3 electrodes, for the meshes 3x3, 4x4 and 5x5, and BC=2

Figure 1 displays the undeformed (solid line) and deformed (dashed line) meshes, for 4x4 finite elements, for BC=1, *pe*=[1, 9].

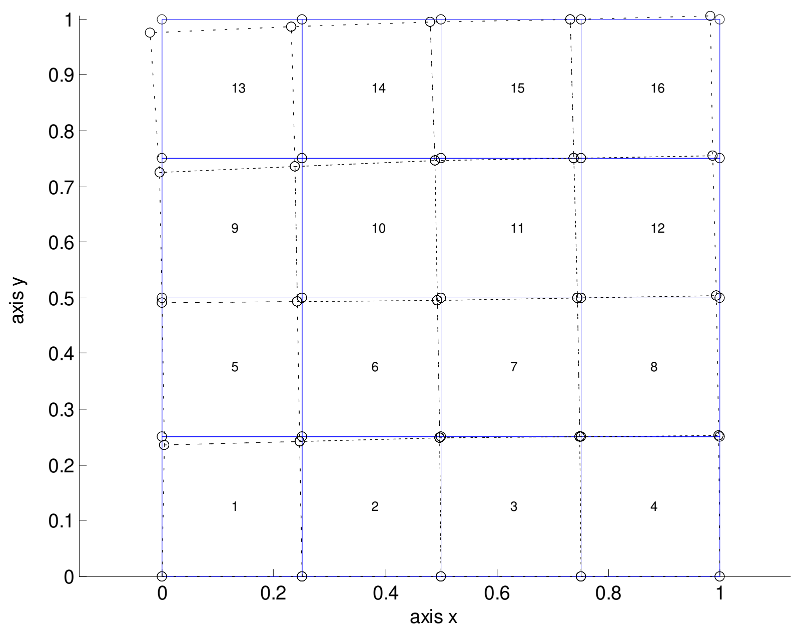

FIGURE 1. Undeformed and deformed meshes, BC=1, *pe*=[1, 9]

In this figure, the element numbers are indicated at the center of the element, the nodemarks are circles, and the node N=21, that is the left vertex on the top side of ω, in finite element 13, is the node with maximum displacement. The deformed mesh corresponds to the tangential displacement u_{tg} of the middle plane ω.

The increase of the displacements with the number of electrodes can also be observed in Tables 5 and 6, for each type of boundary condition. Nevertheless, we have obtained some experiments where this phenomena is not verified, when more than 5 electrodes are considered. In fact, Figure 2 represents the objective function values of the Pareto optimal solutions, for the multi-objective problem (48), with 5x5 finite elements, $m = 25$ and BC=4. These values increase with the number of electrodes, but the Pareto-optimal

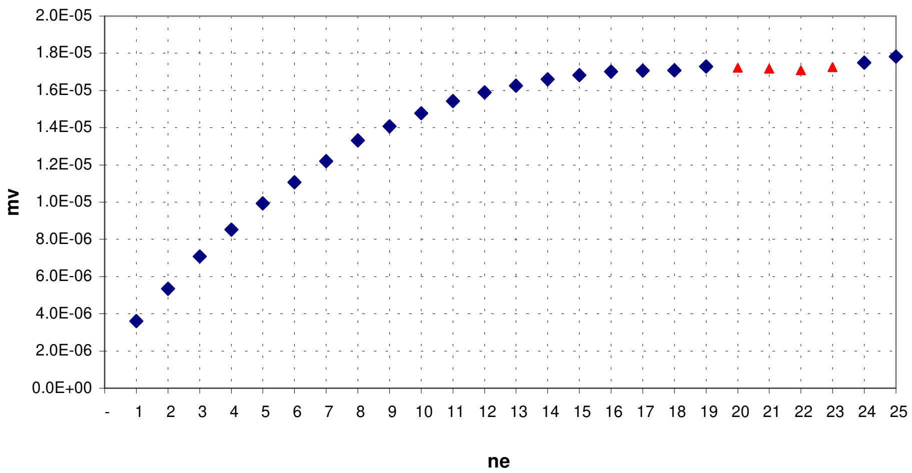

FIGURE 2. Objective values of the Pareto optimal solutions: mesh 5x5, BC=4

number of electrodes is 19 or 25 (to achieve a maximum node displacement it is enough to apply 19 or, even better, 25 electrodes). In fact, the graphic depicted in Figure 2 confirms that for 5x5 finite elements, and the boundary condition BC=4, there is no advantage in considering 20, 21, 22 or 23 electrodes instead of 19, since the actuator effect is better with only 19.

Finally, we have considered nonzero mechanical transverse forces $f_{tv} = \int_{-h}^{+h} f_3\, dx_3 + g_3^+ + g_3^- = 100N$ (cf. (43)) and solved the right linear system in (51), whose unknown is the transverse displacement u_{tv}, for a 3x3 finite element mesh, BC=1 and pe=[1]. Figure 3 represents the graphic of the corresponding discrete electric potential (35), as a function of the thickness variable x_3, for the finite element number 2, and Figure 4 exhibits the corresponding transverse displacement u_{tv} of the middle plane ω of the plate.

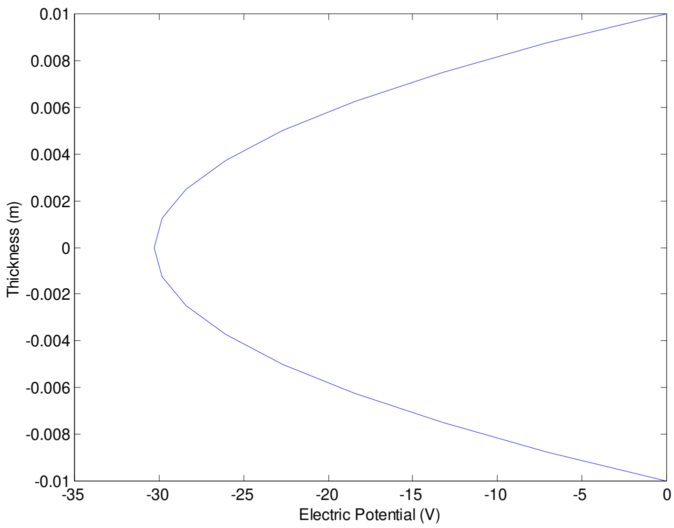

FIGURE 3. Discrete electric potential at finite element 2: mesh 3x3, BC=1, pe=[1]

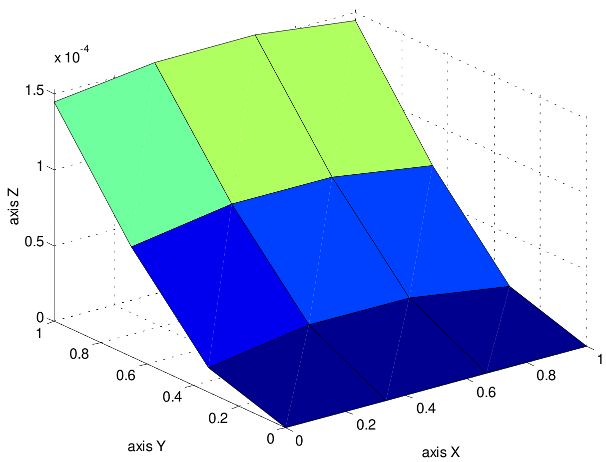

FIGURE 4. Transverse displacement u_{tv} of the middle plane ω: mesh 3x3, BC=1, pe=[1]

5. Conclusion and future work

We have analyzed the actuator effect of the piezoelectric anisotropic plate model (16-19), as a function of the location of the applied electric potentials. The problem is formulated as an integer (single and multi-objective) optimization problem, strongly combinatorial, which has been successfully solved by genetic algorithms. In this paper, a special case of anisotropy was considered, since the modified coefficients $p_{3\alpha\beta}$ and p_{33}, appearing in the model (16-19), and the reduced elastic coefficients $A_{\alpha\beta\gamma\rho}$, chosen in the numerical tests, have been assumed independent of the thickness variable x_3. In a future work we intend to apply the same optimization procedure (that is, genetic algorithms), to study the actuator and sensor effect of a laminated piezoelectric plate. We will consider again the model derived by Figueiredo and Leal [1], but, without imposing that $p_{3\alpha\beta}$, p_{33} and $A_{\alpha\beta\gamma\rho}$ are independent of x_3. In this case, the linear system $Ku = F$ is more complex, since the tangential and transverse displacements are coupled (compare $Ku = F$ in (47) with the two independent linear systems in (51)), and, in addition, the electric potential φ depends, not only, on the transverse displacement (cf. (19) or (35)), but also, on the tangential displacement of the plate. Moreover, in this future work, we will describe in detail all the features of the genetic algorithms applied to solve the problem.

Acknowledgments - This work is partially supported by the project *Mathematical analysis of piezoelectric problems* (FCT–POCTI/MAT/59502/2004 of Portugal), and is part of the project *New materials, adaptive systems and their nonlinearities; modelling, control and numerical simulation* (european community program HRN-CT-2002-00284).

References

[1] I. N. Figueiredo and C. F. Leal, A piezoelectric anisotropic plate model, *Preprint 04-28* Department of Mathematics, University of Coimbra (2004) (paper submitted to International Journal, available in http://www.mat.uc.pt/~isabelf/publica.html).

[2] CALFEM (http://www.byggmek.lth.se/CALFEM), *A finite element toolbox to MATLAB, Version 3.3*, Structural Mechanics and Solid Mechanics, Department of Mechanics and Materials, Lund University, Sweden, 2000.

[3] T. Ikeda, *Fundamentals of Piezoelectricity*, Oxford University Press, New York (1990).

[4] A. Sene, Modelling of piezoelectric static thin plates, *Asymptotic Analysis*, **25**, 1, 1-20 (2001).

[5] P.G. Ciarlet, Basic error estimates for elliptic problems, in *Handbook of Numerical Analysis*, Vol.II (P.G. Ciarlet and J.L. Lions Eds), 17-351, North-Holland, Amsterdam (1991).

[6] D. Goldberg, *Genetic Algorithms in Search, Optimization, and Machine Learning*, Reading, Mass. Addison-Wesley (1989).

[7] K. Deb, *Multi-Objective Optimization using Evolutionary Algorithms*, John Wiley & Sons, England (2001).

[8] L. Costa and P. Oliveira, An elitist genetic algorithm for multiobjective optimization, in *Metaheuristics: Computer Decision-Making*, (M.G.C. Resende and J.P. de Sousa Eds), 217-236, Kluwer Academic Publishers (2003).

[9] L. Costa, L. Fernandes, I. Figueiredo, J. Júdice, R. Leal, and P. Oliveira, Multiple and single objective approaches to laminate optimization with genetic algorithms, *Structural and Multidisciplinary Optimization*, **27**, 1-2, 55-65 (2004).

[10] M. Bernadou and C. Haenel, Modelization and numerical approximation of piezoelectric thin shells. II. Approximation by finite element methods and numerical experiments, *Computer Methods in Applied Mechanics and Engineering*, **192**, 37-38, 4045-4073 (2003).

Lino Costa
Departamento de Produção e Sistemas, Escola de Engenharia, Universidade do Minho, Campus de Azurém, 4800-058 Guimarães, Portugal
E-mail address: lac@dps.uminho.pt
URL: http://sarmento.eng.uminho.pt/dps/lac/

Pedro Oliveira
Departamento de Produção e Sistemas, Escola de Engenharia, Universidade do Minho, Campus de Azurém, 4800-058 Guimarães, Portugal
E-mail address: pno@dps.uminho.pt
URL: http://sarmento.eng.uminho.pt/dps/pno/

Isabel N. Figueiredo
Departamento de Matemática, Universidade de Coimbra, Apartado 3008, 3001-454 Coimbra, Portugal
E-mail address: Isabel.Figueiredo@mat.uc.pt
URL: http://www.mat.uc.pt/~isabelf

Rogério Leal
epartamento de Engenharia Mecânica, Universidade de Coimbra, Pinhal de Marrocos, 3001-201 Coimbra, Portugal
E-mail address: rogerio.leal@dem.uc.pt